Arabian Journal of Chemistry (2020) **13**, 5679–5690

King Saud University

Arabian Journal of Chemistry

www.ksu.edu.sa
www.sciencedirect.com

ORIGINAL ARTICLE

Curcumin-derived one-and two-component organogelators and their performance as template for the synthesis of silver nanoparticles

Balamurugan Rathinam, Zheng-Yung Huang, Bo-Tau Liu *

Department of Chemical and Materials Engineering, National Yunlin University of Science and Technology, Yunlin 64002, Taiwan, Republic of China

Received 23 February 2020; accepted 9 April 2020
Available online 27 April 2020

KEYWORDS

Curcumin derivatives;
Two-component gelators;
Silver nanoparticle;
Cholesteryl derivatives;
Self-assembly;
Hydrogen bonding

Abstract A single-component gelation system based on bis-cholesteryl appended curcumin derivative (**BCC**) and its corresponding two-component organogelation system with sodium stearate (**SS**) was proposed. As a single component gelator, **BCC** forms gel with ethylene diamine (**ED**), through hydrogen bonding between carbonyl group of **BCC** and amino group of **ED** as indicated by temperature dependent solid state NMR (SSNMR) and X-ray diffraction (XRD) profiles. As two-component gelator, **BCC** forms gel with a variety of solvents in the presence of sodium stearate (**SS**). Replacing sodium stearate by other sodium and stearate sources failed to form gel, revealing that both BCC and SS are crucial for effective gelation. The ion-dipole interactions between sodium and keto group of **SS** and **BCC** respectively, as well as π-π interactions confers better gelation abilities to **BCC-SS** system compared to the single component system. The morphology of the as-formed organogels exhibited entangled fibrillated structures and can be regulated by changing the composition of **SS** towards **BCC** and the type of organic solvents. Interestingly, our designed gelator, **BCC-ED** demonstrates potential application as an effective template for the synthesis of silver nanoparticles (AgNPs) at low temperatures as demonstrated by XRD and SEM analysis. Replacing **BCC** or **ED** failed to form AgNPs, revealing the synergistic effect of **BCC-ED**.

1. Introduction

Recently, self-assembly (SA) of small functional molecules into supramolecular structures have become an established technology for the bottom-up fabrication of new materials and nano scale devices (van der Laan et al., 2002; Whitesides and Grzybowski, 2002; Deindörfer et al., 2006; Fialkowski et al., 2006; Shevchenko et al., 2006; Bishop et al., 2009). The self-assembly of large number of individual particles of appropriately chosen properties into high ordered structures such as self-assembled monolayers (Geissler and Xia, 2004), Langmuir-Blodgett films (Whang et al., 2003; Fialkowski

* Corresponding author.
E-mail address: liubo@yuntech.edu.tw (B.-T. Liu).
Peer review under responsibility of King Saud University.

Production and hosting by Elsevier

https://doi.org/10.1016/j.arabjc.2020.04.008
1878-5352

et al., 2006; Tsai et al., 2006) and amphiphilic fibres (Hartgerink et al., 2001) received great industrial applications such as ultrasensitive biosensors (Nam et al., 2003; Bishop et al., 2009), conductive nanowires (Yan et al., 2003), multifunctional textile materials (Sangeetha and Maitra, 2005; Di et al., 2013), drug release (de Loos et al., 2005; George and Weiss, 2006), tissue engineering (Tsai et al., 2006; Zhang et al., 2018), templates for inorganic/organic materials (Terech and Weiss, 1997; Estroff and Hamilton, 2004; Yadav and Ballabh, 2012), opto-electronic and preparation of nano-dimensional inorganic materials (Jung et al., 2003; van Bommel et al., 2003; Džolić et al., 2006). Molecular self-assembly approaches, for example derivatives of peptides used for shape controlled synthesis of metal nanoparticles due to their special features provided by self-assembled templates as well as kinetic aspects which control the formation of nanoparticles of defined size (Slocik et al., 2005; Ray et al., 2006; Vemula and John, 2006; Sahoo et al., 2017. Especially, cholesterol-based low molecular weight organo-gelators (LMWOGs) have attracted a considerable amount of attention because of their versatility in gelation and the diversity of their structures. In our previous report, we studied the self-assembly of mono- and bis-cholesteryl-appended single gel system based on isosorbide (Balamurugan et al., 2016), azobenzene (Balamurugan et al., 2014; Kuo et al., 2017) and pyridine (Rizkiana et al., 2015) conjugates. These gelators are based on single-gel system, in which the gelator molecule immobilizes organic liquids. Hence, in recent years, two-component or multicomponent gelling system received great attention owing to their potential applications in the fields such as pollutant collection (Trivedi and Dastidar, 2006; Zhang et al., 2019), oil spill treatment (Yan et al., 2014; Okesola and Smith, 2016) and advanced materials, due to the possibility of fine-tuning of the gel properties. In detail, the two non-gelling molecules are used to build two-component complex through hydrogen bonding, metal-ligand coordination, acid-base interaction and donor-acceptor interaction. This complex subsequently self-assembles into a fully gelated network via inter-complex interactions (Ye et al., 2015). The structural modification of either of the two components can be adjusted, allowing a fine-tuning of materials behaviour (Hirst and Smith, 2005). Several two or multicomponent gelators are reported in literature, based on the interactions between phthalic acid-alkyl amines (Su et al., 2017), barbituric acid-pyrimidine (Hanabusa et al., 1993), phosphorous based organic acid-amines (Fan et al., 2017), carboxylic acids of dendritic peptides-aliphatic diamines (Partridge et al., 2001), crown ether-diamines (Jung et al., 1999), alkyl cholates-isosorbide (Willemen et al., 2002), bile acids-pyrene (Babu et al., 2003) and bile acids-trinirofluorenone (Maitra et al., 1999). Most of the reported two-component gelators are based on the interaction between carboxylic acids and amines. However, there is no reports on single and two-component gel system based on curcumin-cholesteryl conjugates, i.e. through diketone-amine and ester (linker)-sodium carboxylate respectively.

In this report, we designed a hitherto unreported novel gelator based on curcumin-cholesteryl conjugate (BCC) which act as both single and two-component gelators. **BCC** can form gel only with ED. However, in presence of sodium stearate (**BCC**), **BCC** can gel in a variety of solvents. The gelation ability and structure-property relationships were studied. Curcumin has received considerable attention for its low toxicity and favourable potential in clinical applications including antioxidant, anti-inflammatory, anti-tumor, anti-mutational and anti-HIV properties (Barik et al., 2005; Wu et al., 2010). In addition to that, curcumin can also be used as sensors and reducing agents. Therefore, it was expected that by combining cholesteryl and curcumin unit, the resulting derivative will exhibit attractive properties and can be used for optical or biomedical applications. Therefore, cholesteryl-curcumin based conjugate was designed in this proposed work. **BCC** can form gel with ethylene diamine (ED) and in presence of sodium stearate, **BCC** forms gel with organic solvents such as DMSO, DMF, amines, xylene, toluene, THF, *m*-cresol, 1,2-orthodichloro benzene. In addition, using this versatile gelator **BCC**/**BCC-SS** as stabilizer, water in oil (W/O) gel- emulsions were created, and their morphologies were studied. The morphological and structural analysis of xerogel of **BCC-ED** and **BCC-SS-DMF** were analysed by Scanning Electron Microscopy (SEM) and XRD analysis respectively. The mechanism of aggregation as well as gel formation were proposed. The application of **BCC** as template for synthesis of silver nanoparticle (AgNPs) are discussed in detail. **BCC-ED** gel system play an important role as reducing agent as well as stabilizing/capping agent for the efficient synthesis of pure AgNPs over the other gel systems studied. Reduction of $AgNO_3$ to AgNPs by **BCC-ED** is hitherto unreported. The pure AgNPs synthesized by using **BCC-ED** gel system was characterized by XRD, FT-IR and SEM analysis and discussed in detail.

2. Experimental

2.1. Instruments

All chemicals were purchased from Aldrich Chemicals and were used without further purification. All solvents were purified before use. Fourier transform infrared (FT-IR) spectra were recorded using a Jasco VALOR III Fourier transform infrared spectrophotometer. Nuclear magnetic resonance (NMR) spectra were obtained using a Bruker AMX-400 (Darmstadt, Germany) high-resolution NMR spectrometer, and the chemical shifts were reported in ppm with tetramethylsilane (TMS) as an internal standard. The sample morphologies were characterized using field-emission scanning electron microscopy (FE-SEM, JSM-7001, JEOL, Japan). The xerogel for SEM analysis was prepared by vacuum freeze-drying of the gel formed in the solvent at the critical gelation concentration (CGC) for 12–24 h. The dried samples held on glass substrates were attached to a copper holder for SEM by conductive adhesive tape and were coated with platinum. The X-ray diffraction (XRD) measurements of the xerogel were monitored by Rigaku RINT2000 with a scan rate of 1°/min.

2.2. Gelation test

A pre-calculated weight of gelators (3 mg) and a measured volume of solvent (100 μL) were placed in a glass vial, and the system was heated until all solid materials were dissolved. The solution was then slowly cooled to room temperature, and the test tube was inverted to investigate gel formation. Gel was denoted by G and weak gel was denoted by WG. Systems in which only solution remained throughout the tests were denoted by solution (S). The systems in which the gelator could not be dissolved even at the boiling point of the solvent were considered to be insoluble systems (I). Systems where heating resulted in the dissolution of the gelators and cooling resulted in their precipitation were denoted by P. Unless otherwise mentioned, two-component gels were prepared by mixing 2 mg of **BCC**, 3 mg of sodium stearate and dissolved in DMF. Thus obtained mixture was heated to dissolve, followed by cooling to form gel. For single gel system, 2 mg of **BCC** was added to 100 μL of ED, followed by heating and cooling process leads to form gel. These gels were used to study for the effect of external stimuli such pH, UV, metal ion etc.

2.3. Preparation of Gel-Emulsion

Gel-emulsions were prepared according to the reported procedure[17]. In a typical preparation, 2 mg of the compound **BCC** (and 3 mg of **SS)** was added to a mixture of 0.2 mL of styrene and 0.8 mL of water at room temperature, and the resulting mixture was stirred and slightly heated if necessary to dissolve the compound. Then, the mixture was vigorously shaken by hand for 2 min; finally, a viscous and light yellow emulsion was produced. Formation of the gel-emulsion was confirmed by inverting the test tube to observe whether the mixture inside could still flow. A positive result was obtained when the mixture inside showed no fluidity.

3. Results and discussion

The structure of the individual component used for the gelation such as 1,5-bis (3-methoxy-4-(cholesteryloxycarbony loxy)benzylidene)-2,4-diketopentane (**BCC**), SS and ED are shown in Scheme 1.

The bis-cholesteryl appended curcumin derivative (**BCC**) was synthesized by reacting curcumin with cholesteryl chloroformate in presence of 4-dimethylaminopyridine (DMAP) in dichloromethane. The synthesis procedure and the spectroscopic characterization of **BCC** are provided in supporting information. All spectral data for the synthesized **BCC** corresponded with the structures of the compounds (**Figs. S1 and S2**). The above synthesized **BCC** was found to be soluble in polar solvents such as DMSO, xylene, toluene, DMF, chloroform and chlorobenzene as well as amines such as 1,3-diamino propane, 1,5-diamino pentane and trioctyl amine. **BCC** was found to be insoluble in alcohols of any chain length.

3.1. Gelation properties

The ability of **BCC** to self-assemble was first tested by the formation of organogels in solvents of different polarity, and the results are summarized in Table 1.

The design of **BCC** is structurally similar to $A(LS)_2$ type gelators which consists of cholesteryl (S), benzene (A) and ester groups (L). In the case of $A(LS)_2$ type molecules, the cholesteryl group at the terminal positions have a profound effect on gelation. Therefore, it was expected that **BCC** would exhibit gelation in a variety of solvents. However, **BCC** failed to form gel in any of the organic solvents tested except ethylene diamine (Table 1). Interestingly, **BCC** was found to form gel in a number of solvents in the presence of the surfactant sodium stearate (**SS**) in the ratio of 1:1.5 (**BCC**:**SS**) and 1:2. If the ratio of **BCC:SS** increased over 1:3, it leads to precipitation. The compound SS is a well-known hydrogelator (Zhang and Weiss, 2016). The addition of SS to **BCC** enables gelation in almost all of the solvents in which **BCC** was dissolved (Table 1). Therefore, the structure property relationships of **BCC-ED** and **BCC-SS-**solvents were studied separately and compared.

3.2. BCC-ED gel system

BCC was found to be easily soluble in all amines such as hexyl amine (HA), trioctyl amine (TOA), 1,3-diaminopropane (DAPr), 1,5-diamino pentane (DAP) and diethyl amine (DEA) except ED. However, **BCC** was found to be soluble in ED upon heating. And, gelation was observed while cooling to room temperature. The critical gelation concentration of **BCC-ED** was found to be 20 gL^{-1}. Repeated heating and cooling cycles does not affect the *sol-to-gel* process. Moreover, **BCC** failed to form gel in other amines due to the high solubility of **BCC** at room temperature. This indicates that **BCC** can act as a sensor for the selective detection of ED by selective gelation. The addition of amines to **BCC** leads to colour change from brilliant yellow to reddish brown (Fig. 1). This colour change is due to the keto-enol tautomerism of the curcumin unit in **BCC**. In acidic solution (pH < 7), **BCC** exist in diketone form whereas in basic solution (pH > 7) it exists in enolate form (Fig. S3) (Supharoek et al., 2018).

To gain visual insights regarding the morphology of molecular aggregation modes, BCC-**ED** gel was subjected to SEM analysis, and the results are depicted in Fig. 2.

As observed in SEM images of the xerogels, **BCC-ED** existed as self-assembled fibre-like aggregates with a length of several micrometres and diameter of approximately 100–

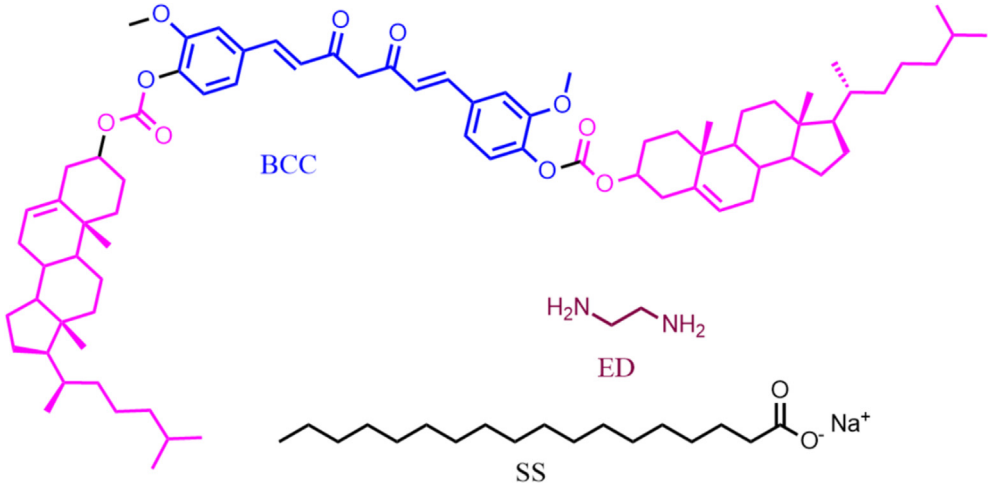

Scheme 1 Structure of the gel components.

Table 1 Gelation properties of BCC and **BCC-SS** in various solvents [G = gel; WG = weak gel; P = precipitate; S = soluble; I = insoluble; GE = gel emulsion].

Solvents/compound	BCC	**BCC + SS**	Solvents/compound	**BCC**	**BCC + SS**
Water	I	**G**	DMF	S	**G**
Methanol	I	I	m-Kresol	S	**G**
Ethanol	I	I	Chloroform	S	**WG**
Propanol	I	I	Acetone	S	P
Butanol	I	I	THF	S	**G**
Octanol	I	I	Ethylene diamine	**G**	**G**
Oleyl amine	I	I	1,3-Diamino propane	S	**G**
Hexanol	I	I	1,5-Diamino pentane	S	**G**
Iso-propanol	I	I	Trioctylamine	S	G
DMSO	S	**G**	Styrene:H_2O	P	**GE**
Xylene	S	**WG**	MMA/*t*-BMA	I	I
Hexylamine	S	**G**	Silicone oil	I	I
Toluène	S	**WG**	Chlorobenzene	S	**WG**

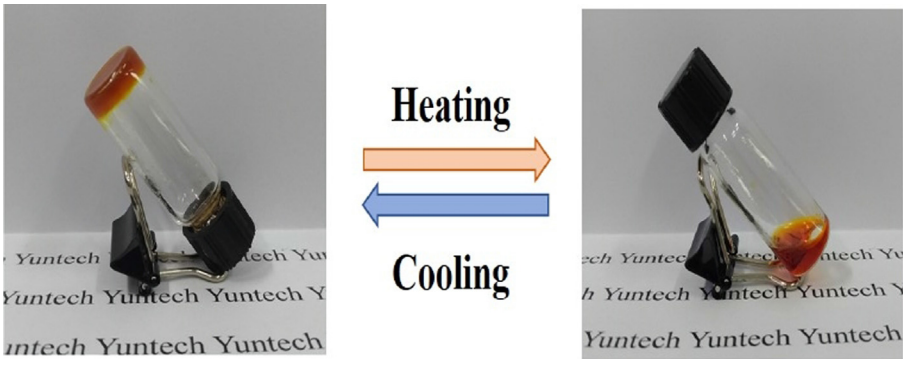

Fig. 1 The digital images of gel-sol process of **BCC-ED** gel.

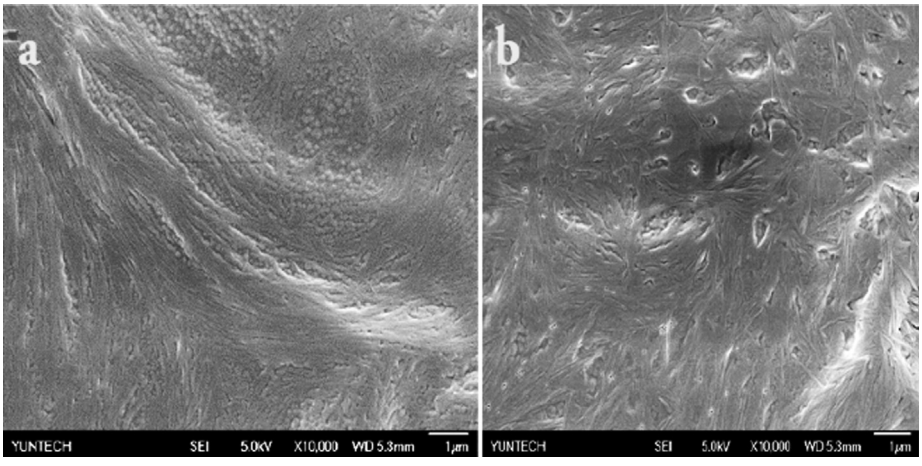

Fig. 2 Representative SEM images of xerogel of **BCC-ED.**

150 nm. The self-assembly of uniform sized nanoparticles and fibrous textures can be observed for **BCC-ED** at CGC (Fig. 2a). However, when increasing the BCC concentration (above CGC), mostly entangled fibrous textures were observed (Fig. 2b). These morphological images revealed that the nanoparticles are interconnected to form fibrous structure at low concentration, which further entangled to form interconnected fibrous structures at higher concentration. The gel-sol transition temperatures (T_{gel}) of the gelators were determined and the concentration dependence T_{gel} values showed that T_{gel} increases with increase in the concentration of gelators (Fig. S4 and Table S1) (Haldar and Karmakar, 2015).

Generally, in LMWGs gel system, temperature-dependent ^{1}H NMR will be recorded in the solvent in which gelators form gel in order to determine the driving forces for the aggregation phenomena as well as the thermo-reversibility of the gels. Since the gelling solvent (ED) could not be used as NMR solvent in this case, solid state NMR was performed for **BCC-ED** at various temperatures and the results are merged in Fig. 3.

From the spectra, it was observed that the peak at 195 ppm corresponding to carbonyl group (—C═O; carbon "**a**" in the figure) of the curcumin unit is broad at 303 K. However, with increasing temperature from 303 K to 323 K, the peak was found to be sharp and sharpness increased when the temperature was further increased to 333 K. This indicates that **BCC-ED** remained in gel state at low temperature (303 K) and converted to solution state when increasing temperature to 333 K. This revealed the occurrence of a *gel-to-sol* phase transition with increase in temperature. It may be due to the breaking of secondary forces, which in this case is the hydrogen bonding between amine of ethylene diamine and diketo group of curcumin unit. Similar sharpness of the peaks was observed along with slight shifting of peaks in almost all of the peaks with increase in temperature. For example, the peak at 165.3 ppm corresponding to —O—C(═O)—O—Ch* was shifted to 164.6 when increasing the temperature from 303 K to 333 K, which indicated that carbonyl (in ester) group is involved in gel formation. Similarly, the peaks at 142.6 ppm corresponding to —C═CH— in curcumin unit, 134.7 ppm corresponding to ArC—O—C═O, 113.1 ppm corresponding to ArC and 56.7 ppm corresponding to methoxy carbon were shifted to 142.2, 134.4, 113.5 and 58.1 ppm, respectively suggesting that these functional groups are involved in the self- assembly of BCC in the presence of ethylene diamine. Moreover, the peak at 75.1 ppm corresponding to cholesteryl carbon attached to oxygen shifted to 74.6 ppm and then to 73.6 ppm while increasing the temperature to 323 K and 333 K respectively. These results indicated that the cholesteryl unit is involved in gel formation. Based on these evidences, it is understood that the aromatic carbons, cholesteryl carbons and hydrogen bonding between curcumin diketo groups with ethylene diamine are responsible for the gelation properties of BCC.

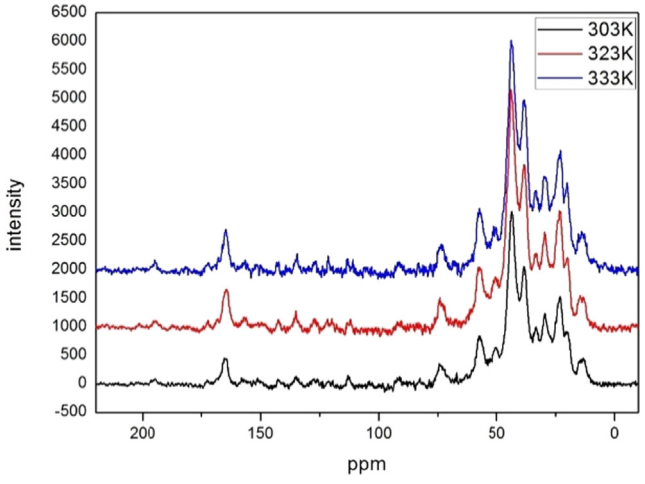

Fig. 3 Temperature-dependent SSNMR spectra of **BCC-ED** gel.

Furthermore, it suggested that the cholesteryl-cholesteryl interaction (van der Waals forces), π-π stacking as well as hydrogen bonding between the amino groups of ED with the carbonyl group of curcumin unit played an important role for the formation of gel. Instead of diketo group of curcumin, there is another possibility of hydrogen bonding between carbonyl group (ester; linker) and amine. However, the structure and length of the molecule by XRD analysis and simulation studies matches with the structure which undergo hydrogen bonding through diketo group of curcumin. Based on these results, the mechanism of gel formation of BCC with ethylene diamine was proposed and the schematic representation of the proposed mechanism was shown in Fig. 4.

To gain visual insights into the molecular packing, the xerogel of **BCC-ED** was subjected to XRD analysis, and the results are depicted in Fig. 5. According to the Bragg lattice diffraction formula, $n\lambda = 2d \sin\theta$, where λ is the wavelength and $n = 1$. XRD was operated with a copper excitation wavelength of 0.154 nm to determine the incident angle θ and the layer spacing d. Using the data, the formula produced an obvious peak for **BCC** at $2\theta = 1.81$ and $d = 4.88$ nm. **BCC-ED** exhibited peak at $2\theta = 2.16$, and $d = 4.08$ nm. These interlayer distances were found to coincide with the results obtained from the molecular simulation software (Fig. 6).

3.3. BCC-SS gel system in different solvent

The compound BCC in the presence of SS formed gel in polar solvents such as DMF, DMSO, *m*-cresol and low polar solvents such as xylene, toluene, dichlorobenzene, THF etc. (Table 1). Amines such as ethylene diamine, hexyl amine, 1,3-diaminopropane, 1,5-diaminopentane and trioctyl amine also form gel with BCC-SS. Unlike BCC, BCC-SS can form gel in all the amines studied, indicating that BCC-SS cannot act as a sensor for ED. The gel colour varied from pale yellow to dark yellow and reddish brown or brown depending on the solvents. The colour of the gels had no apparent change during repeated heating and cooling cycles (Fig. 7). Unlike other amines, trioctyl amine shows dark yellow colour, whereas all other amines exhibited dark reddish brown. All the gels were found to be semi-transparent except THF and trioctyl amine based gels, which were opaque. All the gels exhibited excellent thermo-reversibility, which means that the compounds could be brought into solution by heating and the hot solution could be converted back to the gels upon cooling to room temperature. This cycle could be repeated several times.

From the Table 1, it was observed that BCC-SS did not form gel in alcohols, oleylamine and in monomers, such as tertiary butyl methacrylate (*t*-BMA) and methyl methacrylate (MMA). In addition to that, **BCC-SS** form gel emulsion in water and styrene mixture after heating and cooling process; whereas BCC forms precipitate in styrene. To investigate the effect of the water content on the phase behaviour of the gel-emulsions, **BCC-SS**/water/styrene with different water contents, including 0, 20, 40, 60, 70, 80, 90 and 100% (v/v) was studied. The systems with $>50\%$ water did not form gel, whereas all other proportions of $< 50\%$ water formed gels. In addition to that, styrene alone (100% styrene) did not form gel in the absence of water (Fig. S5). This could be due to the insoluble nature of BCC in water.

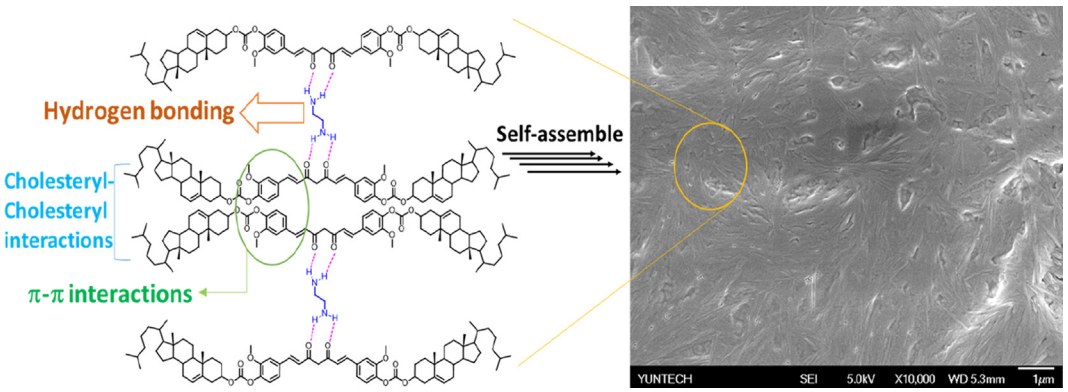

Fig. 4 Schematic representations of aggregation of **BCC** in **ED.**

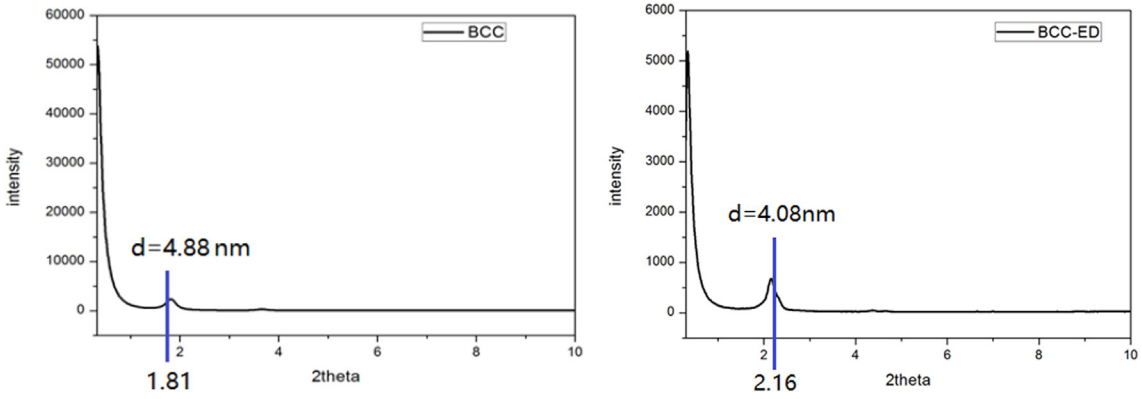

Fig. 5 XRD diffraction patterns of (a) **BCC** and (b) **BCC-ED.**

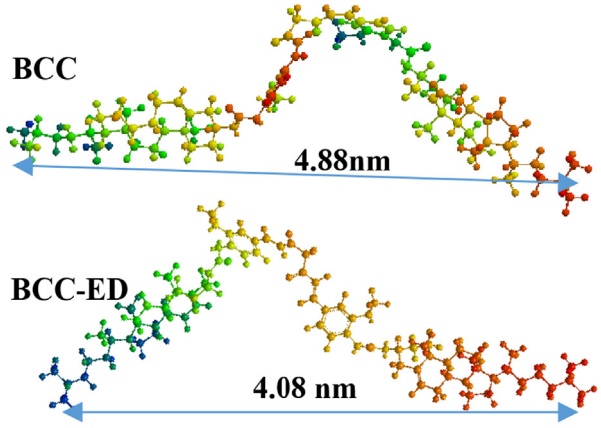

Fig. 6 The simulated molecular models of BCC and **BCC-ED**.

3.4. Morphological studies

To gain visual insights regarding the morphologies of the molecular aggregation modes, all the gelators were subjected to SEM analysis, and the representative images are depicted in Fig. 8 and Fig. S6. As observed in the SEM images of the xerogels, the **BCC-SS** gels in various solvents exhibited self-assembled, one-dimensional, fibre-like aggregates with length of several micrometres and diameter of approximately 100–200 nm. These xerogels undergo further entanglement to form bundles of fibrous aggregates. The nanostructures of the xerogels in different solvents are significantly different, and the morphology of the aggregates vary from fibre and rod to wrinkled texture with the change of solvents. This morphology is structurally similar to our previously reported morphology for bis-cholesteryl appended isosorbide based gelator systems (Balamurugan et al., 2016). It may be due to the fact that both are structurally $A(LS)_2$ type, in which only A is different.

For example, the xerogel of BCC in xylene and 1,2-dichlorobenzene exhibited long range fibrous structures whereas chloroform and 1,5-diamino pentane exhibited short range dense fibrous structures (Fig. 8a-d). The structure of xerogel of BCC in DMF resembles the structure of xylene (Fig. S6c). In the case of 1,2-dichlorobenzene gel system, the self-assembly of uniform spherical spheres connected to each other in a linear fashion and formed a fibrous structure. The arrangement of spherical spheres can be seen clearly in Fig. 8b. The size of each sphere is roughly measured as 20 nm, and therefore nearly 4 to 6 nanoparticle join in a linear way forming 100 nm length fibre as observed in Fig. 8b **(**Fig. S8-d**)**. Fig. 8e and 8 h corresponds to the gelation ability of **BCC** and **BCC-SS** in styrene/water (1:1; v/v), respectively. BCC fail to form gel or gel-emulsion in styrene/water (1:1; v/v), and precipitation was observed. This was further supported by morphological analysis of the same by SEM, which exhibited uniform size spherical nano-spheres as shown in

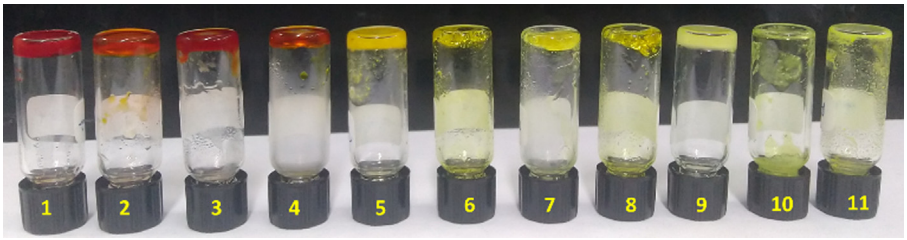

Fig. 7 Representative digital images of gels of **BCC-SS** in (1) hexylamine; (2) 1,5-diamino pentane; (3) 1,3-diamino propane; (4) m-cresol, (5) Trioctyl amine; (6) Toluene, (7) Chlorobenzene; (8) xylene; (9) THF; (10) Acetone and (11) chloroform.

Fig. 8e. However, in the presence of SS, BCC can form gel-emulsion in styrene/water (1:1; v/v), and resulted in randomly arranged short-range dense fibrous structure as seen in SEM images (Fig. 8h). Hence, increasing water content more than 50% in styrene/water mixture leads to turbidity, which may be due to the non-aqueous solubility of BCC.

In order to determine the efficiency of sodium stearate, it was replaced by other sources of sodium as well as stearate and the gelation abilities with BCC was analysed. Replacing sodium stearate by other stearates such as stearic acid and iron stearate leads to precipitate formation. Similarly replacing sodium stearate by other sodium sources such as sodium oxalate, sodium thiocyanate, sodium lauryl sulphate (SLS) and sodium acetate were performed in DMF. Among these, sodium thiocyanate forms gel (Fig. 8f and Fig. S7) whereas others failed to form gel. However, sodium thiocyanate did not form gel in the absence of BCC, which indicates that in the BCC-SS gel system in DMF, the BCC is not just bound by SS. The BCC and SS cooperatively combined and formed gel.

In addition, the ratio of SS also affects the aggregation mode of BCC-SS gel system. The gel system containing **BCC-SS** (1:2) in xylene exhibited fibrous structure (Fig. 8a). However, when increasing the concentration of SS in **BCC-SS** (1:3 wt%) in xylene exhibited sheet like structure (Fig. S6e).

Heating of gel samples is known to result in an increase of gelator ^{1}H NMR signals due to disaggregation of the gel network into smaller, dissolvable aggregates observable by NMR (Džolić et al., 2006). To study the formation and the thermos-reversibility of the gels, the temperature-dependency of the ^{1}H NMR spectra was investigated for BCC-SS (1:1.5; wt %) in DMSO d_6 and the results are presented in Fig. S8. As shown in the spectra, when increasing the temperature from 303 K to 363 K, a significant up field shifting occurred for the proton signals at 7.3 ppm, corresponding to aromatic protons (curcumin unit in BCC), which revealed that aromatic protons are involved in aggregation.

Generally, in two component system, H-bonding plays an important role in gel formation (Willemen et al., 2002; Hirst and Smith, 2004). However, H-bonding is not commonly seen in the case of sodium stearate (SS). SS [$CH_3(CH_2)_{16}COONa$] is an ionic compound and its organic part contains polar groups. Therefore, dipole-dipole, ion-dipole interactions as well as van der Waals forces are the possible/available driving forces for gel formation. So it is assumed that there is additional possibility of ion-pole interactions between sodium (SS) and carbonyl group (—C═O) of the curcumin unit. Therefore, the existence of π-π interaction as well as ion-dipole interaction might be the base for gel formation at room temperature (303 K). However, the exact mechanism of gel formation is unclear since the non-covalent interactions between molecules are subtle and sometimes hard to understand (Raeburn and Adams, 2015). When increasing the temperature from 303 K to 363 K, the *gel* → *sol* transition occurred, which may have been due to the breaking of ion-dipole interaction, which in turn disrupted the gel state. Increasing the temperature caused disruptions in the supramolecular arrangement and decreased the effects of the secondary forces (the disruption of intermolecular forces between the two molecules).

3.5. Effect of external stimuli towards the stability of the gels

The stability of the gels over external stimuli such as pH (acid-base reaction), sonication and UV irradiation were studied. **BCC/BCC-SS** failed to form gel in any solvents in the presence of sonication (without heating) as well as UV irradiation. Similarly, the gel formed by heating and cooling process was not affected by sonication/UV irradiation; instead, the gel became stronger after sonication than freshly prepared gels. This result indicated that the phase transitions could not be tuned by sonication. However, it improved the stability of the gel to some extent. The addition of acid (acetic acid) to the **BCC-ED** or **BCC-SS** gel in DMF turned the colour of the gel to yellow with precipitation. However, addition of base (TEA) resulted in colour change to brown, but failed to form gel. These results indicate that gel-to-sol can be tuned by acid; hence gel cannot be retained by addition of base.

Since curcumin forms complexes via its β-diketone moiety with almost all the metal ions (Wanninger et al., 2015; Călinescu et al., 2019), the influence of the metal ions for example Cu^{2+}, Fe^{3+}, Hg^{2+}, Pd^{2+}, Ni^{2+} and Zn^{2+} towards the stability of **BCC-ED/BCC-SS** (in DMF) gels were tested. With progressive addition of approximately 10 equivalents of these cations to the gels resulted in precipitation after heating and cooling process. This may be due to the selective complexation of these metal ions with the diketone group of BCC, separating/breaking the forces between BCC and ED or BCC and SS, which leads to precipitation (Fig. S9).

3.6. Potential application of BCC based gelators as a template for silver nanoparticles (AgNPs) synthesis

In general, the organo/hydro gelators can be used as a template or support for the synthesis of nanoparticles such as silver nanoparticle (AgNP), gold nanoparticles (AuNPs) and iron nanoparticles (FeNPs). Since the gelator possess 3D-network structure, a large number of functional groups can

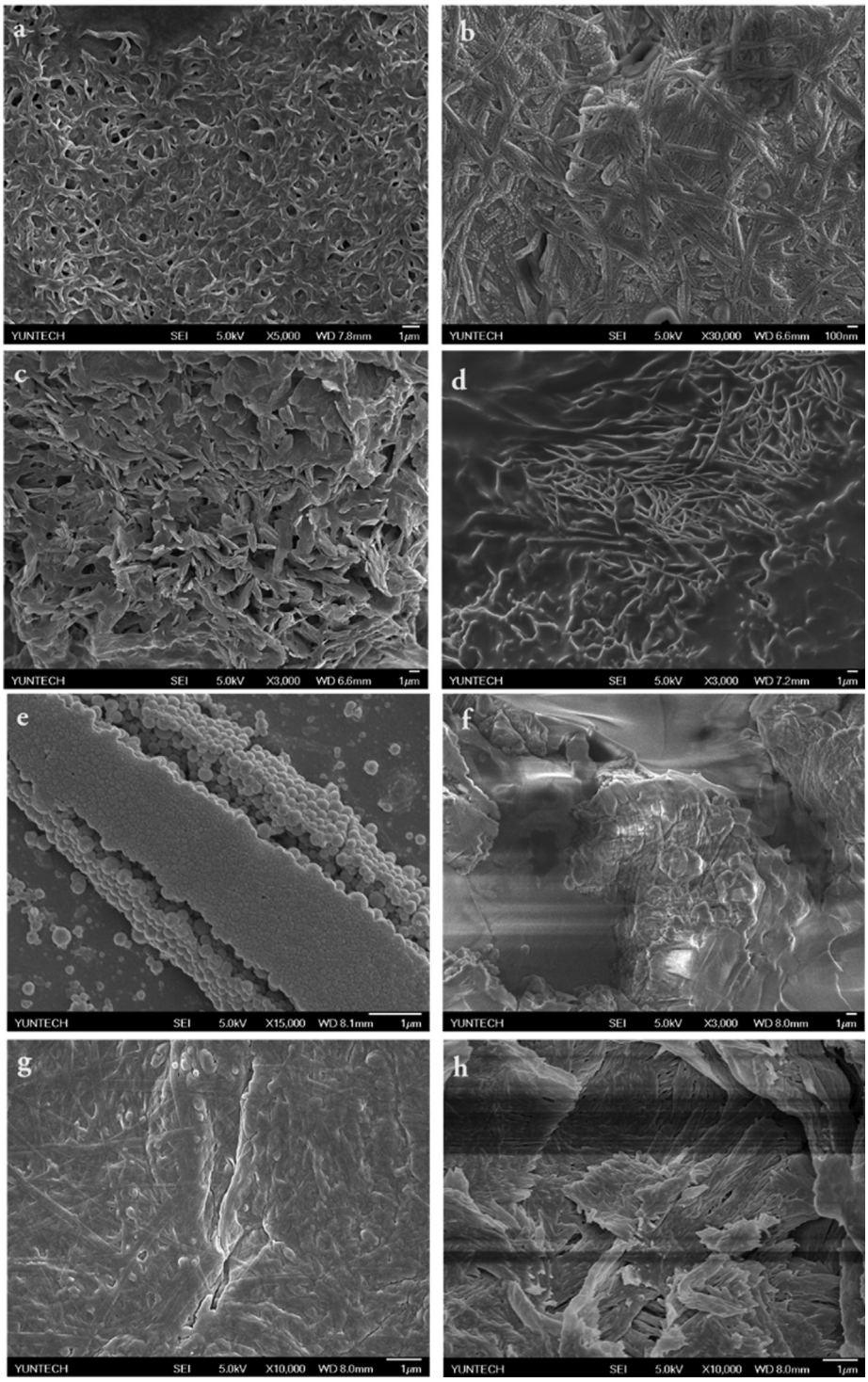

Fig. 8 Representative SEM images of **BCC-SS** in (a) Xylene; (b) 1,2-dichlorobenzene; (c) Chloroform; (d) 1,5-diaminopentane; (e) BCC + Styrene/H_2O(1:1); (f) sodium thiocyanate (g) SS in dilute water (h) BCC-SS-styrene xerogel.

provide space for the nucleation and growth of the noble metal nanoparticles (Wu et al., 2015; Zhu et al., 2019). Therefore, we attempted to use our gelators as template/structure directing agent for the synthesis of AgNPs.

Here, we used three different gel system as templates for the synthesis of AgNPs as follows: (1) **BCC-ED** gel; (ii) **BCC-SS-DMF** gel and (iii) **SS-DMF** gel. Once the above gels were prepared, an equal amount of $AgNO_3$ was added directly into the gel in each case and the resulting mixture was heated again to 80 °C for 20–30 min and cooled to room temperature. In all cases, gel state was retained. However, the colour of the gels turned to dark brown/ brownish black along with formation of silver mirror (Zaier et al., 2017) as shown in Fig. 9.

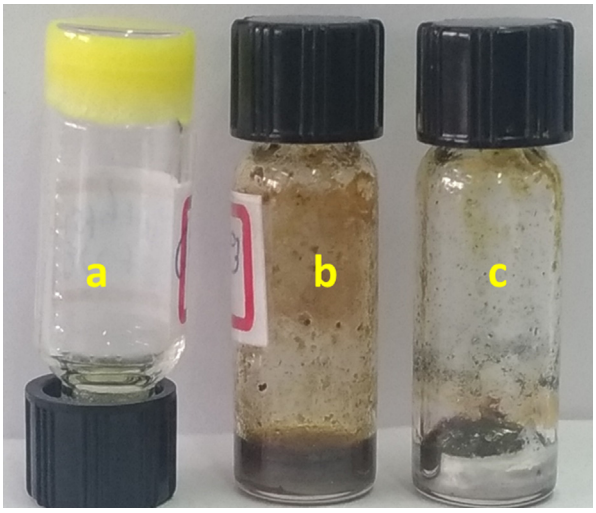

Fig. 9 Digital images of gels obtained from (a) BCC-SS gel; (b) **BCC-ED** + $AgNO_3$ and (c) SS-DMF-$AgNO_3$.

From the Fig. 9, the deposition of Ag can be seen at the bottom of the vials due to the presence of sodium metal (Na^+) which undergo reduction reaction with $AgNO_3$ (Fig. 9). However, the stability of the gel was not affected by metal ions (Fig. S10). The appearance of silver formation can be seen in the vial by naked eye (Fig. 9). The resulting gels were diluted by adding excess DMF and centrifuged. The DMF was decanted and the deposits were washed by using additional acetone and centrifuged. The acetone was decanted and the resulting powder was allowed to dry at vacuum oven at room temperature. AgNPs can be separated from the template by dissolving template in chloroform/dichloromethane. The samples were subjected to XRD analysis and the results are merged in Fig. 10.

The XRD patterns for the synthesized AgNPs by different templates are merged in Fig. 10. When comparing the XRD pattern of **BCC-ED**, the templates containing SS such as BCC-SS-DMF gel as well as SS-DMF gel system exhibited peaks at the 2θ value of $< 35°$. These peaks are attributed to the formation of silver stearate as shown in Fig. 11. The formation of silver stearate was further verified by the morphological analysis by SEM, optical microscope and FT-IR

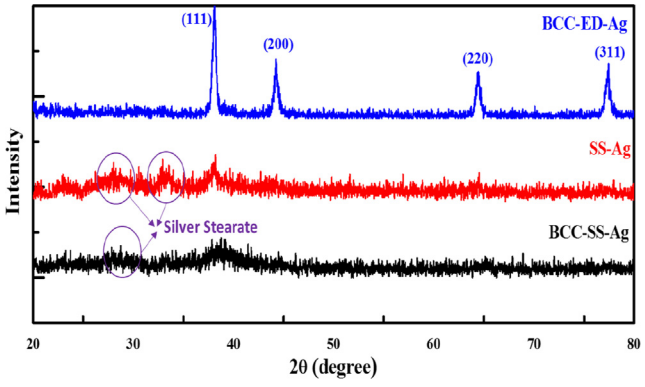

Fig. 10 The XRD patterns of synthesized AgNPs via different template.

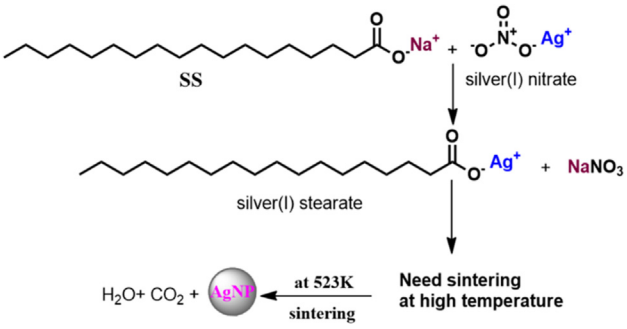

Fig. 11 The formation of silver stearate.

analysis. The FT-IR spectra of AgNPs synthesized by different templates are shown in Fig. S11 (see supporting information). From the spectra, it was observed that the peaks around 1515 and 1415 cm^{-1} corresponding to υ_{as} (COO) and υ_s(COO) vibration peaks for the ester present in silver stearate (Mao et al., 2019). The morphological analysis of silver stearate by SEM exhibited layered structures as shown in Fig. 12**,** which resembles other reported structure (Lee et al., 2003). The silver stearate exhibited platelet crystals of layer textures under optical microscope (Fig. S12), which is in accordance with the reported textures (Lin et al., 2004). AgNPs can be seen clearly from the top view of the sample **BCC-ED**-Ag placed over SEM substrate/carbon tape (Fig. S12d) The synthesis of AgNPs from silver stearate was reported previously (Mao et al., 2019), in which silver stearate was subjected to sintering at 523k leading to partial decomposition of silver stearate, producing silver stearate coated AgNPs. We can apply the same protocol for the production of AgNPs, if necessary. This means that, silver stearate, which is obtained from gels containing sodium stearate should undergo high temperature sintering and AgNPs thus obtained will be coated with silver stearate (Mao et al., 2019). Therefore, obtaining pure AgNPs is a tedious process and novel methods/reagents are in demand for the efficient production of pure NPs.

Interestingly, without addition of sodium stearate and without forming silver stearate, AgNPs were successfully synthesized by using **BCC-ED** gel system, especially at very low temperature (80 °C). The XRD pattern of thus obtained AgNPs exhibited peaks at 2θ values of 38°, 44°, 64° and 77°, respectively corresponding to (1 1 1), (2 0 0), 220 and (3 1 1) planes (Fig. 10). This XRD pattern is in accordance with the structure of Ag(0) reported in literature (Mu et al., 2013; Anandalakshmi et al., 2016; Mao et al., 2019). However, the gel system without ED (BCC-SS-DMF gel) and without BCC (SS-DMF gel) failed to form well resolved XRD pattern of Ag(0). These results indicated the importance of BCC as well as ED for the successful formation of AgNPs.

The morphological analysis of thus obtained AgNPs exhibited spherical nano-spheres with the size of 60–100 nm (Fig. 13). The morphology of AgNPs were found to be in accordance with the reported literature (Mu et al., 2013; Anandalakshmi et al., 2016). These results suggested that the template based on BCC and ED (**BCC-ED** gel) played an important role in the formation of AgNPs. The silver nitrate appears to be reduced by **BCC-ED** gel resulting in AgNPs without adding any other reagents, indicating that **BCC-ED** act as reducing agent as well as capping/stabilizing agent for

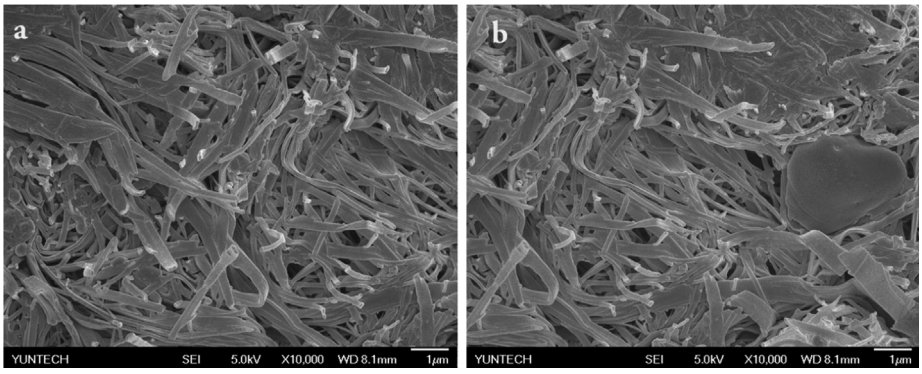

Fig. 12 SEM images of silver stearate.

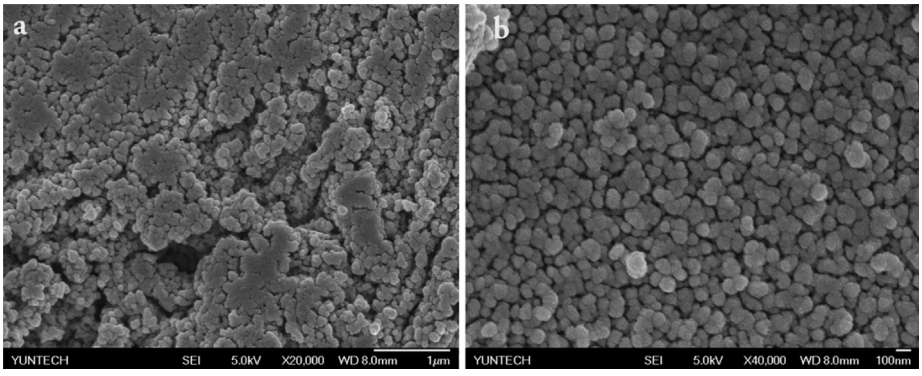

Fig. 13 The representative SEM images of AgNPs obtained from **BCC-ED** gel (different magnifications).

the synthesis of AgNPs. It is acceptable since, curcumin was reported as reducing agent (Tønnesen and Greenhill, 1992; Safavi et al., 2017) for the reduction of Fe^{3+} to Fe^{2+} (Tønnesen and Greenhill, 1992) as well as for $AgNO_3$ (Yang et al., 2016). The presence of the diketo-moiety in BCC structure seems to be essential both in redox reactions and in the scavenging of oxygen radicals (Tønnesen and Greenhill, 1992).

Although BCC-SS-DMF gel contains the reducing agent BCC, the reduction of $AgNO_3$ by sodium from SS takes place predominantly over the reduction by curcumin unit of BCC. Therefore, BCC-SS-DMF gel failed to produce AgNPs at this stage. In order to produce AgNPs, it should undergo further reaction such as sintering at high temperature and purification steps are needed. These results revealed that BCC produce AgNPs in the presence of ED. In addition, the reduction reaction by **BCC-ED** used very low temperature (80 °C) and the template can be effortlessly removed by non-gelling solvent such as dichloromethane or chloroform and can be reused. These results revealed that **BCC-ED** acts as the best reducing agent/template for the synthesis of AgNPs from $AgNO_3$. Hence, **BCC-ED** gel system is a highly potential platform for the efficient synthesis of AgNPs.

4. Conclusions

In summary, we successfully designed and develped a novel single and two-component gelation system derived from curcumin-cholesteryl conjugates (**BCC**). The driving force for gel formation in **BCC-ED** and **BCC-SS** in solvents are thought to proceed with H-bonding and ion-dipole interactions, respectively. Depending on the type of solvent as well as changes in the composition of SS with respect to BCC, the morphology can be tuned. Regarding the potential applications, BC-ED can be used as an effective template for the synthesis of pure AgNPs. Replacing BCC or ED in **BCC-ED** gel system by sodium stearate or other solvents respectively failed to form AgNPs. These evidences proved that the gel system **BCC-ED** acts as an efficient reducing agent and stabilizing/capping agent for the synthesis of pure AgNPs at low temperature. The present investigation is a perspective to provide new clues about the designing of gelators for the fabrication of nanomaterials for the potential application of conductive nanomaterials. This report may afford a specific approach to understand the soft matter and design of new nanomaterials.

Declaration of Competing Interest

The authors declare that they have no known competing financial interests or personal relationships that could have appeared to influence the work reported in this paper.

Acknowledgements

The authors thank the Ministry of Science and Technology, Taiwan, Republic of China for financially supporting this research under Contract no. MOST 107-2622-E-224-001-CC3.

Appendix A. Supplementary material

Supplementary data to this article can be found online at https://doi.org/10.1016/j.arabjc.2020.04.008.

References

Anandalakshmi, K., Venugobal, J., Ramasamy, V., 2016. Characterization of silver nanoparticles by green synthesis method using pedalium murex leaf extract and their antibacterial activity. Appl. Nanosci. 6 (3), 399–408.

Babu, P., Sangeetha, N.M., Vijaykumar, P., Maitra, U., Rissanen, K., Raju, A.R., 2003. Pyrene-derived novel one- and two-component organogelators. Chem. A Eur. J. 9 (9), 1922–1932.

Balamurugan, R., Kai-Ming, W., Chien, C.-C., Liu, J.H., 2014. Structure–property relationships of symmetrical and asymmetrical azobenzene derivatives as gelators and their self-assemblies. Soft Matter 10 (44), 8963–8970.

Balamurugan, R., Zhang, Y.S., Fitriyani, S., Liu, J.H., 2016. Click chemistry-assisted, bis-cholesteryl-appended, isosorbide-based, dual-responsive organogelators and their self-assemblies. Soft Matter 12 (23), 5214–5223.

Barik, A., Mishra, B., Shen, L., Mohan, H., Kadam, R.M., Dutta, S., Zhang, H.-Y., Priyadarsini, K.I., 2005. Evaluation of a new copper (ii)–curcumin complex as superoxide dismutase mimic and its free radical reactions. Free Radical Biol. Med. 39 (6), 811–822.

Bishop, K.J.M., Wilmer, C.E., Soh, S., Grzybowski, B.A., 2009. Nanoscale forces and their uses in self-assembly. Small 5 (14), 1600–1630.

Călinescu, M., Fiastru, M., Bala, D., Mihailciuc, C., Negreanu-Pîrjol, T., Jurcă, B., 2019. Synthesis, characterization, electrochemical behavior and antioxidant activity of new copper(ii) coordination compounds with curcumin derivatives. J. Saudi Chem. Soc. 23 (7), 817–827.

De Loos, M., Feringa, B.L., Van Esch, J.H., 2005. Design and application of self-assembled low molecular weight hydrogels. Eur. J. Org. Chem. 2005 (17), 3615–3631.

Deindörfer, P., Geiger, T., Schollmeyer, D., Ye, J.H., Zentel, R., 2006. Semicarbazides as gel forming agents for common solvents and liquid crystals. J. Mater. Chem. 16 (4), 351–358.

Di, Y., Hong, W., Dai, J., 2013. Investigation of self-assembly of two-component organogel system based on trigonal acids and aminobenzothiazole derivatives. J. Nanomater. 2013, 5.

Džolić, Z., Wolsperger, K., Žinić, M., 2006. Synergic effect in gelation by two-component mixture of chiral gelators. New J. Chem. 30 (10), 1411–1419.

Estroff, L.A., Hamilton, A.D., 2004. Water gelation by small organic molecules. Chem. Rev. 104 (3), 1201–1218.

Fan, K., Wang, X., Han, G., Niu, L., Yang, X., Yin, Z., Song, J., 2017. Two-component organogels of phosphorous-based organic acids and diamine. Soft Mater. 15 (3), 247–253.

Fialkowski, M., Bishop, K.J.M., Klajn, R., Smoukov, S.K., Campbell, C.J., Grzybowski, B.A., 2006. Principles and implementations of dissipative (dynamic) self-assembly. J. Phys. Chem. B 110 (6), 2482–2496.

Geissler, M., Xia, Y., 2004. Patterning: Principles and some new developments. Adv. Mater. 16 (15), 1249–1269.

George, M., Weiss, R.G., 2006. Molecular organogels. Soft matter comprised of low-molecular-mass organic gelators and organic liquids. Acc. Chem. Res. 39 (8), 489–497.

Haldar, S., Karmakar, K., 2015. A systematic understanding of gelation self-assembly: Solvophobically assisted supramolecular gelation via conformational reorientation across amide functionality on a hydrophobically modulated dipeptide based ambidextrous gelator, n-n-acyl-(l)val-x(obn), (x = 1, ω-amino acid). RSC Adv. 5 (81), 66339–66354.

Hanabusa, K., Miki, T., Taguchi, Y., Koyama, T., Shirai, H., 1993. Two-component, small molecule gelling agents. J. Chem. Soc., Chem. Commun. 18, 1382–1384.

Hartgerink, J.D., Beniash, E., Stupp, S.I., 2001. Self-assembly and mineralization of peptide-amphiphile nanofibers. Science 294 (5547), 1684–1688.

Hirst, A.R., Smith, D.K., 2004. Solvent effects on supramolecular gel-phase materials: Two-component dendritic gel. Langmuir 20 (25), 10851–10857.

Hirst, A.R., Smith, D.K., 2005. Two-component gel-phase materials—highly tunable self-assembling systems. Chem. A Eur. J. 11(19), 5496–5508.

Jung, J.H., Lee, S.-H., Yoo, J.S., Yoshida, K., Shimizu, T., Shinkai, S., 2003. Creation of double silica nanotubes by using crown-appended cholesterol nanotubes. Chem. A Eur. J. 9 (21), 5307–5313.

Jung, J.H., Ono, Y., Shinkai, S., 1999. Organogels of azacrown-appended cholesterol derivatives can be stabilized by host-guest interactions. TetrahedronLett. 40 (48), 8395–8399.

Kuo, S.-Y., Liu, C.-Y., Balamurugan, R., Zhang, Y.-S., Fitriyani, S., Liu, J.H., 2017. Dual-responsive als-type organogelators based on azobenzene–cholesteryl conjugates and their self-assemblies. New J. Chem. 41 (24), 15555–15563.

Lee, S., Han, S., Kim, K., 2003. Controlled growth of layered silver stearate on 2d and 3d surfaces. ETRI J. 25, 517–522.

Lin, B., Dong, J., Whitcomb, D.R., Mccormick, A.V., Davis, H.T., 2004. Crystallization of silver stearate from sodium stearate dispersions. Langmuir 20 (21), 9069–9074.

Maitra, U., Vijay Kumar, P., Chandra, N.J., D'souza, L., Prasanna, M.D., Raju, A.R., 1999. First donor–acceptor interaction promoted gelation of organic fluids. Chem. Commun. (7), 595–596.

Mao, Y., Xi, L., Deng, Q., Wang, S., 2019. Preparation of ag nanoparticles coated with silver stearate for low-temperature sinter-bonding. J. Electron. Mater. 48, 3336–3344.

Mu, F., Zhao, Z., Zou, G., Bai, H., Wu, A., Liu, L., Zhang, D., Norman Zhou, Y., 2013. Mechanism of low temperature sintering-bonding through in-situ formation of silver nanoparticles using silver oxide microparticles. Mater. Trans. 54 (6), 872–878.

Nam, J.-M., Thaxton, C.S., Mirkin, C.A., 2003. Nanoparticle-based bio-bar codes for the ultrasensitive detection of proteins. Science 301 (5641), 1884–1886.

Okesola, B.O., Smith, D.K., 2016. Applying low-molecular weight supramolecular gelators in an environmental setting – self-assembled gels as smart materials for pollutant removal. Chem. Soc. Rev. 45 (15), 4226–4251.

Partridge, K.S., Smith, D.K., Dykes, G.M., Mcgrail, P.T., 2001. Supramolecular dendritic two-component gel. Chem. Commun. 4, 319–320.

Raeburn, J., Adams, D.J., 2015. Multicomponent low molecular weight gelators. Chem. Commun. 51 (25), 5170–5180.

Ray, S., Das, A.K., Banerjee, A., 2006. Smart oligopeptide gels: In situ formation and stabilization of gold and silver nanoparticles within supramolecular organogel networks. Chem. Commun. 26, 2816–2818.

Rizkiana, M.F., Balamurugan, R., Liu, J.H., 2015. The effect of meta versus para substitution on the aggregation of bis-cholesteryl appended 2,6-disubstituted pyridine-based gelators. New J. Chem. 39 (8), 6068–6075.

Safavi, M.S., Shojaosadati, S.A., Yang, H.G., Kim, Y., Park, E.J., Lee, K.C., Na, D.H., 2017. Reducing agent-free synthesis of curcumin-loaded albumin nanoparticles by self-assembly at room temperature. Int. J. Pharm. 529 (1), 303–309.

Sahoo, J.K., Roy, S., Javid, N., Duncan, K., Aitken, L., Ulijn, R.V., 2017. Pathway-dependent gold nanoparticle formation by biocatalytic self-assembly. Nanoscale 9 (34), 12330–12334.

Sangeetha, N.M., Maitra, U., 2005. Supramolecular gels: Functions and uses. Chem. Soc. Rev. 34 (10), 821–836.

Shevchenko, E.V., Talapin, D.V., Kotov, N.A., O'brien, S., Murray, C.B., 2006. Structural diversity in binary nanoparticle superlattices. Nature 439 (7072) 55–59.

Slocik, J.M., Stone, M.O., Naik, R.R., 2005. Synthesis of gold nanoparticles using multifunctional peptides. Small 1 (11), 1048–1052.

Su, T., Hong, K.H., Zhang, W., Li, F., Li, Q., Yu, F., Luo, G., Gao, H., He, Y.-P., 2017. Scaleable two-component gelator from phthalic acid derivatives and primary alkyl amines: Acid–base interaction in the cooperative assembly. Soft Matter 13 (22), 4066–4073.

Supharoek, S.-A., Ponhong, K., Siriangkhawut, W., Grudpan, K., 2018. Employing natural reagents from turmeric and lime for acetic acid determination in vinegar sample. J. Food Drug Anal. 26 (2), 583–590.

TcNnesen, H.H., Greenhill, J.V., 1992. Studies on curcumin and curcuminoids. Xxii: Curcumin as a reducing agent and as a radical scavenger. Int. J. Pharmaceutics 87(1), 79–87.

Terech, P., Weiss, R.G., 1997. Low molecular mass gelators of organic liquids and the properties of their gels. Chem. Rev. 97 (8), 3133–3160.

Trivedi, D.R., Dastidar, P., 2006. Instant gelation of various organic fluids including petrol at room temperature by a new class of supramolecular gelators. Chem. Mater. 18 (6), 1470–1478.

Tsai, P.-S., Yang, Y.-M., Lee, Y.-L., 2006. Fabrication of hydrophobic surfaces by coupling of langmuir−blodgett deposition and a self-assembled monolayer. Langmuir 22 (13), 5660–5665.

Van Bommel, K.J.C., Friggeri, A., Shinkai, S., 2003. Organic templates for the generation of inorganic materials. Angew. Chem. Int. Ed. 42 (9), 980–999.

Van Der Laan, S., Feringa, B.L., Kellogg, R.M., Van Esch, J., 2002. Remarkable polymorphism in gels of new azobenzene bis-urea gelators. Langmuir 18 (19), 7136–7140.

Vemula, P.K., John, G., 2006. Smart amphiphiles: Hydro/organogelators for in situ reduction of gold. Chem. Commun. 21, 2218–2220.

Wanninger, S., Lorenz, V., Subhan, A., Edelmann, F.T., 2015. Metal complexes of curcumin – synthetic strategies, structures and medicinal applications. Chem. Soc. Rev. 44 (15), 4986–5002.

Whang, D., Jin, S., Wu, Y., Lieber, C.M., 2003. Large-scale hierarchical organization of nanowire arrays for integrated nanosystems. NANO Lett. 3 (9), 1255–1259.

Whitesides, G.M., Grzybowski, B., 2002. Self-assembly at all scales. Science 295 (5564), 2418–2421.

Willemen, H.M., Vermonden, T., Marcelis, A.T.M., Sudhölter, E.J.R., 2002. Alkyl derivatives of cholic acid as organogelators: One-component and two-component gels. Langmuir 18 (19), 7102–7106.

Wu, F.-Y., Sun, M.-Z., Xiang, Y.-L., Wu, Y.-M., Tong, D.-Q., 2010. Curcumin as a colorimetric and fluorescent chemosensor for selective recognition of fluoride ion. J. Lumin. 130 (2), 304–308.

Wu, X.-Q., Wu, X.-W., Huang, Q., Shen, J.-S., Zhang, H.-W., 2015. In situ synthesized gold nanoparticles in hydrogels for catalytic reduction of nitroaromatic compounds. Appl. Surf. Sci. 331, 210–218.

Yadav, P., Ballabh, A., 2012. Synthesis, characterization and nanoparticles synthesis using a simple two component supramolecular gelator: A step towards plausible mechanism of hydrogelation. Colloids Surf., A 414, 333–338.

Yan, H., Park, S.H., Finkelstein, G., Reif, J.H., Labean, T.H., 2003. DNA-templated self-assembly of protein arrays and highly conductive nanowires. Science 301 (5641), 1882–1884.

Yan, L., Li, G., Ye, Z., Tian, F., Zhang, S., 2014. Dual-responsive two-component supramolecular gels for self-healing materials and oil spill recovery. Chem. Commun. 50 (94), 14839–14842.

Yang, X.X., Li, C.M., Huang, C.Z., 2016. Curcumin modified silver nanoparticles for highly efficient inhibition of respiratory syncytial virus infection. Nanoscale 8 (5), 3040–3048.

Ye, F., Chen, S., Dong Tang, G., Zhen Wu, B., Ma, M., Qin Shi, Y., Wang, X., 2015. Synthesis of two-component dendritic gelators and their self-assembly behavior in mma. Mater. Sci. Forum 815, 551–556.

Zaier, M., Vidal, L., Hajjar-Garreau, S., Balan, L., 2017. Generating highly reflective and conductive metal layers through a light-assisted synthesis and assembling of silver nanoparticles in a polymer matrix. Sci. Rep. 7 (1), 12410.

Zhang, J., Liu, J., Tong, C., Chen, S., Zhang, B., Zhang, B., Song, J., 2019. Smart materials for environmental remediation based on two-component gels: Room-temperature-phase-selective gelation for the removal of organic pollutants including nitrobenzene/o-dichlorobenzene, and dye molecules from the wastewater. Nanoscale Res. Lett. 14 (1), 42.

Zhang, M., Weiss, R.G., 2016. Self-assembled networks and molecular gels derived from long-chain, naturally-occurring fatty acids. J. Braz. Chem. Soc. 27, 239–255.

Zhang, S., Xing, M., Li, B., 2018. Biomimetic layer-by-layer self-assembly of nanofilms, nanocoatings, and 3d scaffolds for tissue engineering. Int. J. Mol. Sci. 19 (6), 1641.

Zhu, J., Wang, R., Geng, R., Zhang, X., Wang, F., Jiao, T., Yang, J., Bai, Z., Peng, Q., 2019. A facile preparation method for new two-component supramolecular hydrogels and their performances in adsorption, catalysis, and stimuli-response. RSC Adv. 9 (39), 22551–22558.